Applied Physics Letters

RESEARCH ARTICLE | JANUARY 14 2025

Impact of a RbF post-deposition treatment on the chemical structure of wide-gap $CuIn_{0.1}Ga_{0.9}Se_2$ thin-film solar cell absorber surfaces

Luisa Both ; Dirk Hauschild ; Mary Blankenship ; Ralph Steininger ; Wolfram Witte ; Dimitrios Hariskos ; Stefan Paetel ; Michael Powalla; Clemens Heske ; Lothar Weinhardt

Appl. Phys. Lett. 126, 021603 (2025)
https://doi.org/10.1063/5.0239968

Applied Physics Letters ARTICLE pubs.aip.org/aip/apl

Impact of a RbF post-deposition treatment on the chemical structure of wide-gap $CuIn_{0.1}Ga_{0.9}Se_2$ thin-film solar cell absorber surfaces

Cite as: Appl. Phys. Lett. **126**, 021603 (2025); doi: 10.1063/5.0239968
Submitted: 23 September 2024 · Accepted: 20 December 2024 ·
Published Online: 14 January 2025

View Online Export Citation CrossMark

Luisa Both,[1,2] Dirk Hauschild,[1,2,3,a)] Mary Blankenship,[1,2,3] Ralph Steininger,[2] Wolfram Witte,[4] Dimitrios Hariskos,[4] Stefan Paetel,[4] Michael Powalla,[4,5] Clemens Heske,[1,2,3] and Lothar Weinhardt[1,2,3]

AFFILIATIONS

[1]Institute for Chemical Technology and Polymer Chemistry (ITCP), Karlsruhe Institute of Technology (KIT), Kaiserstr. 12, 76131 Karlsruhe, Germany
[2]Institute for Photon Science and Synchrotron Radiation (IPS), Karlsruhe Institute of Technology (KIT), Kaiserstr. 12, 76131 Karlsruhe, Germany
[3]Department of Chemistry and Biochemistry, University of Nevada, Las Vegas (UNLV), 4505 Maryland Parkway, Las Vegas, Nevada 89154-4003, USA
[4]Zentrum für Sonnenenergie- und Wasserstoff-Forschung Baden-Württemberg (ZSW), Meitnerstraße 1, 70563 Stuttgart, Germany
[5]Light Technology Institute (LTI), Karlsruhe Institute of Technology (KIT), Kaiserstr. 12, 76131 Karlsruhe, Germany

[a)]**Author to whom correspondence should be addressed:** dirk.hauschild@kit.edu

ABSTRACT

A detailed characterization of the impact of a RbF post-deposition treatment (RbF-PDT) on the chemical structure of a wide-gap Cu(In, Ga)Se_2 thin-film solar cell absorber surface with a high Ga/(Ga + In) (GGI) ratio of 0.9 is presented. Using synchrotron- and lab-based x-ray photoelectron spectroscopy, as well as x-ray-excited Auger electron spectroscopy, we observe distinct differences to RbF-PDT on absorber surfaces with the common GGI of ∼0.3. In particular, RbF-PDT reduces sodium and oxide content at the surface, while the copper concentration at the surface is not affected. We find no spectral evidence for the formation of a distinct Rb–In–Se surface layer. In addition, we observe that the GGI ratio at the surface is slightly decreased due to a reduction of the Ga and an increase in the In concentration, which may explain the observed improvement in the power conversion efficiency after the PDT (from 6.8% to 7.3%).

Currently, Cu(In,Ga)$(S,Se)_2$-based thin-film solar cells with a "standard" Ga/(Ga + In) (GGI) ratio of ∼0.3 achieve the highest power conversion efficiencies (PCEs) among all stable thin-film solar cells, i.e., above 23% on a laboratory scale.[1–3] Such high efficiencies have been achieved using alkaline fluoride (NaF, KF, RbF, or CsF) post-deposition treatments (PDTs).[4–12] To deliberately control and optimize their effects, understanding the mechanism of PDTs is an important and ongoing topic of discussion. It has been found that a RbF-PDT significantly reduces charge carrier recombination, both in the Cu(In, Ga)Se_2 (CIGSe) absorber bulk and at the buffer/CIGSe interface, which is accompanied by an improvement of the open-circuit voltage (V_{OC}).[4,5,13] This improvement is sometimes attributed to the formation of a Rb–In–Se surface layer at the absorber surface,[14–16] while other publications did not find such surface species for high-performing devices.[7,8,17] Wider bandgap CIGSe devices, achieved by increasing the absorber's GGI, have attracted strong research interest, as they promise higher V_{OC} and can serve as possible candidates for top cells in tandem devices.[18,19] However, wide bandgap devices only reach efficiencies far below the detailed-balance limit[20,21] due to a large V_{OC} deficit ($E_{Gap}/e - V_{OC}$),[22,23] mainly caused by interfacial recombination that is typically ascribed to a strong cliff in the conduction band alignment,[24–26] thus limiting the PCE.

Combining high GGI CIGSe absorbers with PDTs is thus a potentially promising route to increase the PCE. In fact, NaF- and KF-PDTs have been shown to improve efficiencies with CIGSe absorbers up to a GGI of 0.8.[27,28] However, according to Refs. 16 and 19 no benefit from NaF-, KF-, and/or RbF-PDTs have been reported for In-free $CuGaSe_2$ absorbers. It was suggested that the presence of In is essential for

beneficial effects of the PDT,[16,29] and that the overall changes induced by alkali-PDT strongly depend on the group III composition.[11]

In an earlier study, we have used a combination of ultraviolet photoelectron and inverse photoemission spectroscopy (UPS and IPES, respectively) to *directly* investigate the electronic structure of a RbF-PDT CIGSe absorber with an integral GGI of 0.9 and its interface with a CdS buffer layer. We found a substantial cliff in the conduction band alignment (−0.53 eV),[30] while flat conduction band alignments were found for high-performance solar cells with a GGI ∼0.3 and 0.7.[31] Building on this, our present study investigates the impact of the RbF-PDT treatment on the *chemical* structure of the same wide-gap CIGSe absorbers (i.e., with a bulk GGI ratio of 0.9) using synchrotron-based hard x-ray photoelectron spectroscopy (HAXPES), laboratory-based x-ray photoelectron spectroscopy (XPS), as well as x-ray induced Auger electron spectroscopy (XAES).

The CIGSe absorber samples used in this study were prepared at the ZSW, using an industry-relevant in-line process described in detail in Ref. 32. The absorber layers were grown with an integral GGI ratio of 0.9 and a Cu/(Ga + In) ratio of 0.7 by co-evaporation of Cu, In, Ga, and Se in a multi-stage process onto Mo-coated soda-lime glass substrates. The thickness of the CIGSe absorber is 2.3 μm as determined by x-ray fluorescence analysis. Typically, Na[33,34] and some K[35,36] diffuse at elevated temperatures from the alkali-containing glass into the absorber. Afterward, the processed absorber samples were separated into two pieces. The first piece was subjected to a RbF-PDT[4,10] (in the following "PDT"), while the second did not ("no PDT"). By breaking the vacuum, both samples were then shortly exposed to air and rinsed in a 1.5M ammonia solution to remove surface contaminations, e.g., formed oxides and surplus RbF. The CIGSe absorbers were immediately sealed under inert atmosphere. "Sister" samples of the same batch (i.e., with the same rinsing procedure) were processed to full solar cells using a solution-grown CdS buffer, a sputtered i-ZnO high-resistive layer, and a ZnO:Al window layer. They showed a median PCE of 6.8% and a V_{oc} of 790 mV, a fill factor (FF) of 67.1%, and a short-circuit current density (J_{SC}) of 13.2 mA/cm^2 for no PDT. After PDT, these values improve to 7.3% and 820 mV, with a FF of 66.1%, and a J_{SC} of 13.6 mA/cm^2 with PDT. Similar-processed cells with a GGI of ∼0.3 typically achieve PCEs of 17%–18%.[32] At KIT, the samples were introduced into the surface characterization system of the Materials for Energy (MFE) laboratory via an argon-filled glovebox without any further air exposure.[37] This surface characterization system is equipped with an O micrometer Argus CU electron analyzer, a non-monochromatized O micrometer DAR450 twin anode x-ray source (Mg K_α and Al K_α), and a monochromatized SIGMA Surface Science MECS x-ray source (Al K_α). After the initial XPS and XAES measurements, the samples were transferred to the X-SPEC beamline[38] at the KIT Light Source with a short air exposure (less than 30 s) for HAXPES measurements. The X-SPEC beamline is an undulator beamline with a unique energy range from 68 eV to 16 keV and is equipped with a SPECS Phoibos 225 electron analyzer. The MFE electron spectrometer was calibrated using sputter-cleaned copper, silver, and gold foils.[39] The HAXPES binding energy was calibrated using the Au 4f photoemission line.[39] The higher excitation energy used in HAXPES leads to a higher kinetic energy of the corresponding electron as compared to laboratory-based XPS. Hence, the characteristic inelastic mean free path λ increases for, e.g., the Ga 3d/In 4d peaks from 2.3 (Mg K_α XPS) to 3.5 nm ($h\nu = 2.1$ keV HAXPES).[40,41]

Figure 1 shows HAXPES survey spectra of the no PDT (black) and the RbF-PDT (red) CIGSe surfaces, excited with 2.1 keV. All expected absorber elements can be detected. Furthermore, we find signals from surface adsorbates (i.e., C and O) and alkali metals (i.e., Na and Rb), while K and F are not detected. Due to the high GGI, all Ga lines are very prominent, while the In lines are low in intensity. After RbF-PDT, the C 1s intensity remains almost unchanged. In contrast, the intensity of the O 1s peak is reduced by a factor of approximately two.

Upon RbF-PDT, the prominent lines of Cu, Ga, and Se remain at approximately the same intensity (e.g., Cu $2p_{3/2}$: ∼3% decrease, Ga $2p_{3/2}$: ∼4% decrease, and Se 3d: ∼3% increase), while the In lines (e.g., In $3d_{5/2}$) increase in intensity by approximately 22% after RbF-PDT. This is in contrast to several reports on narrow-gap absorbers, where Cu (and Ga) lines were often found to be strongly reduced or even completely removed after PDT.[10,42–45]

To investigate the chemical environment of the alkali elements (Rb and Na) present at the CIGSe surface, Fig. 2 shows the Rb $2p_{3/2}$ and Na 1s detail spectra. In literature, the Rb 3d peaks are frequently analyzed for this purpose.[8,15,46] However, for high GGI samples, this is not reliable due to the energetic overlap of the (strong) Ga 3p and the (weak) Rb 3d signals [see discussion of Fig. 4(a)]. Hence, we investigate the Rb $2p_{3/2}$ peak, which can only be accessed using hard x-ray excitation, displayed in Fig. 2(a). While the no PDT sample shows no evidence of Rb at the surface (as expected), a distinct Rb $2p_{3/2}$ line is observed for the PDT sample. The absolute Rb 2p intensity is very small (see Fig. 1) and will be analyzed in detail later. The Rb $2p_{3/2}$ is fitted using a linear background and one Voigt function, giving a binding

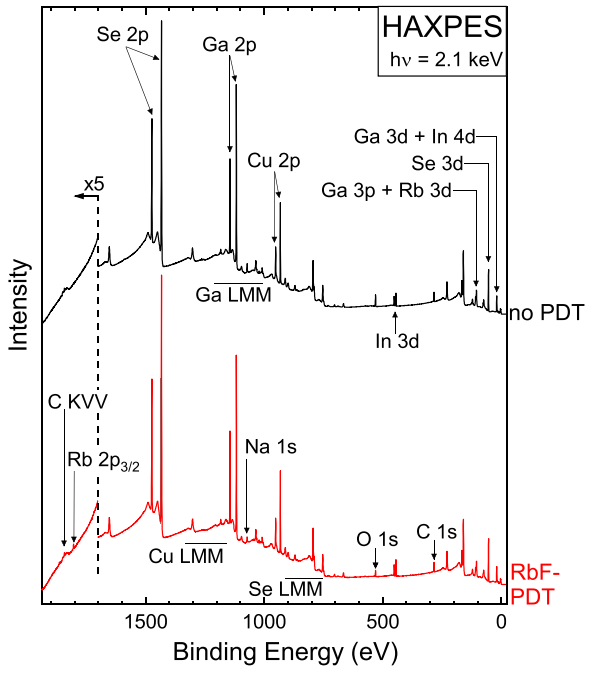

FIG. 1. 2.1 keV-excited HAXPES survey spectra of the no PDT (black) and RbF-PDT (red) $CuIn_{0.1}Ga_{0.9}Se_2$ absorber. The spectra are magnified (x5) in the binding energy region above 1700 eV. Prominent photoemission lines and spectral regions with Auger signals are labeled.

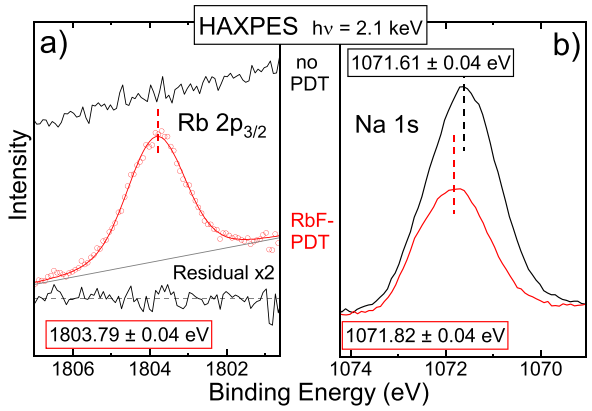

FIG. 2. (a) Rb $2p_{3/2}$ and (b) Na 1s HAXPES spectra for the no PDT (black) and RbF-PDT (red) $CuIn_{0.1}Ga_{0.9}Se_2$ absorbers. The Rb $2p_{3/2}$ PDT data (red circles) are shown together with a fit using a linear background and a Voigt function (red continuous line); the magnified (×2) residual is shown below. The peak energies are highlighted by dashed vertical lines and in the respective black and red boxes.

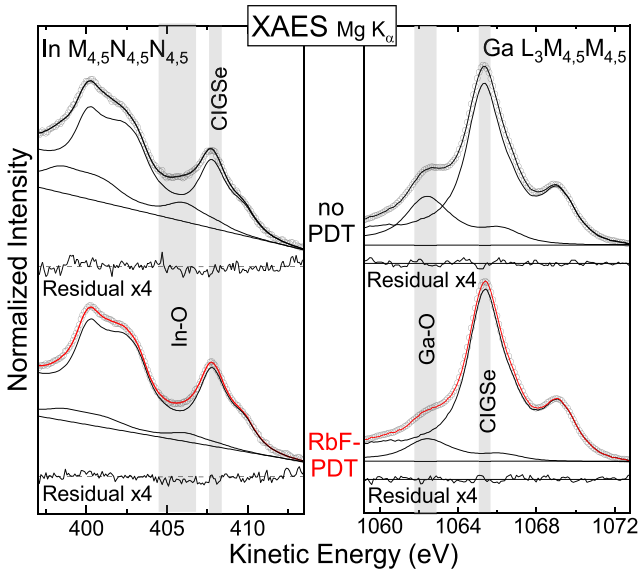

FIG. 3. Mg K_α-excited In MNN (left) and Ga LMM (right) XAES spectra for the no PDT and RbF-PDT $CuIn_{0.1}Ga_{0.9}Se_2$ absorbers. Experimental data are shown as gray circles, individual species (fit components) are represented in black, and the fit sum is displayed in red and black for the PDT and no PDT absorber, respectively. The fit residuals are magnified by a factor of four and shown below each spectrum. Literature values of most prominent peaks for different chemical environments are depicted as vertical gray bars.[8,39,53–55]

energy of 1803.79 ± 0.04 eV, which closely matches results for Rb at CIGSe surfaces with a GGI = 0.3.[47,48] As we will show later in this paper, we find no evidence for the formation of a Rb–In–Se surface layer at the investigated surface.

For both CIGSe surfaces, Na is detected [Fig. 2(b)]. The intensity of the Na 1s peak decreases by a factor of approximately two after the RbF-PDT. A decrease in the Na content after PDT was also detected for absorbers with a GGI = 0.3 and was associated with a replacement of lighter (Na) by heavier (Rb) alkalis at the surface.[4] In addition to the change in peak intensity, a peak shift from 1071.61 to 1071.82 (±0.04) eV is found. Both are typical values found for Na on CIGSe surfaces with lower GGI and without PDT steps.[8,49–52] The shift cannot be explained by a change in band bending (see below), and thus we relate it to a slight PDT-induced change in the chemical environment of Na.

To determine the chemical environment of In and Ga at the absorber surface, the In $M_{4,5}N_{4,5}N_{4,5}$ and Ga $L_3M_{4,5}M_{4,5}$ XAES spectra are analyzed in Fig. 3. After PDT, the In MNN exhibits a slightly deeper "valley" at 405.5 eV, while the Ga LMM Auger shows a decrease in the shoulder at 1062 eV. To quantify these spectral changes, we fit the spectra using a linear background and two respective single-species components. The single-species spectra still have a complex peak shape, consisting of many different Auger transitions, and were taken from an Ar^+-ion cleaned GGI = 0.3 CIGSe absorber from ZSW (measured with the same experimental settings). The component representing the oxidic environment was additionally convoluted with a Gaussian width of 1.0 ± 0.1 eV as an additional fitting parameter to account for slight variations in the chemical environment. For both PDT and no PDT, the prominent In $M_{4,5}N_{4,5}N_{4,5}$ component at 407.82 ± 0.04 eV (PDT) and at 407.81 ± 0.04 eV (no PDT) is in accordance with In in a CIGSe environment.[8,54] The weaker second component at 406.22 ± 0.04 eV (PDT) and 406.05 ± 0.04 eV (no PDT) matches literature values for In in an oxidic environment [e.g., In $(OH)_3$ or In_2O_3].[39,53] The fraction of In in an oxidic environment, i.e., In–O/(In–O + In(CIGSe)), decreases from 23% for no PDT to 11% for PDT. In a similar fashion, the Ga LMM spectra exhibit the main component at 1065.37 ± 0.04 eV (no PDT) and 1065.42 ± 0.04 eV (PDT), corresponding to Ga in a CIGSe environment.[54] The second component at 1062.42 ± 0.04 eV (no PDT) and 1062.45 ± 0.04 eV (PDT) indicates Ga in an oxidic environment.[53,55,56] The fraction of Ga in an oxidic environment, i.e., Ga–O/(Ga–O + Ga(CIGSe)), is reduced from 25% for no PDT to 13% for PDT. A reduction of In and Ga (hydr)oxides was similarly observed for 0.3 GGI CIGSe absorber surfaces after PDTs,[45,48] which could be beneficial for the later buffer layer/absorber interface.[12]

To further study the impact of RbF-PDT, we investigate the Rb 3d/Ga 3p, Se 3d, and Ga 3d/In 4d regions, as depicted in Figures 4(a), 4(b), and 4(c), respectively. The spectra are normalized to the peak area. Upon PDT, all absorber-related lines shift slightly (∼0.1 eV) to lower binding energies. To compensate this shift, the plotted PDT spectra were shifted to higher binding energies by the values given in Fig. 4. The fact that all lines exhibit a similar shift suggests that the RbF-PDT induces a small change in surface band bending. While an additional downward band bending was found for GGI = 0.3 absorbers after PDT,[7] our data indicate that the RbF-PDT slightly shifts the bands *upward* for high GGI absorbers.

For the Ga 3p/Rb 3d region, the presence of the Rb 3d signal is visible in the PDT spectrum as a minimal intensity increase at ∼111 eV on the high binding energy side of the Ga 3p spectrum (with respect to the no PDT spectrum). Note that the Rb 2p photoemission line shown in Fig. 2(a) unambiguously verifies that Rb is present at the CIGSe surface. To analyze the spectral changes, the difference spectrum (PDT minus no PDT) is plotted below the spectra. We find two peaks between 109.5 and 112.0 eV, with the characteristic Rb 3d spin–orbit splitting of 1.5 eV.[39] The binding energy of Rb $3d_{5/2}$

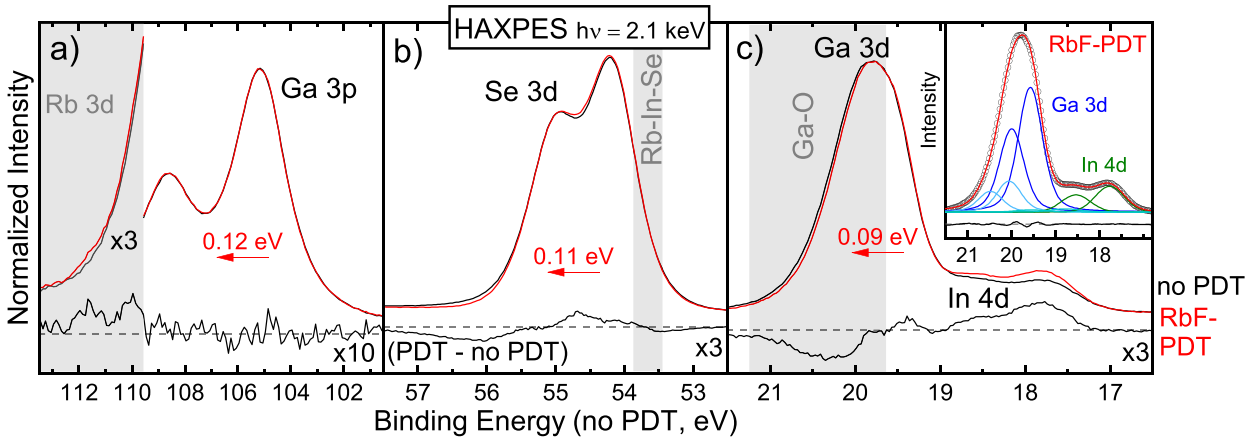

FIG. 4. (a) Ga 3p/Rb 3d, (b) Se 3d, and (c) Ga 3d/In 4d HAXPES spectra of the no PDT (black) and RbF-PDT (red) $CuIn_{0.1}Ga_{0.9}Se_2$ absorbers, excited with 2.1 keV. The binding energy region above 109.5 eV is magnified by a factor of 3. The inset in (c) shows the fit of the Ga 3d/In 4d PDT spectrum, with the fit residual shown underneath. All spectra were normalized to the peak area and the PDT spectra were shifted, as indicated by the red arrows, to better highlight spectral differences. The difference spectra (PDT–no PDT) are plotted below the respective spectra in gray and magnified by the noted factors.

(110.0 ± 0.1 eV) matches reported values for Rb incorporated in CIGSe, i.e., no separate (Cu- and Ga-free) Rb–In–Se bonding environment.[15] To calculate the Rb/Ga ratio, we use the spectral intensity of the difference spectrum between 109.5 and 112.0 eV, assigned to Rb 3d, and of the no PDT spectrum, assigned to "pure" Ga 3p. Taking the respective photoionization cross sections into account,[57] we derive a Rb/Ga ratio of 0.005 ± 0.003. The error bar arises from the very weak Rb 3d signal and the reduction of Ga-oxides due to the RbF-PDT. The binding energy of Se $3d_{5/2}$ to indicate a potential Rb–In–Se type surface species (as reported in some cases after PDT of standard GGI chalcopyrite absorber surfaces) would be expected around 53.7 eV, shown by the region shaded in gray.[14–16] For the here-studied high-GGI absorber, no additional intensity is found in this region; furthermore, a *narrowing* of the Se 3d line is found, reflected in the negative intensity at approximately 53.5 and 56 eV. The narrowing found for the PDT samples could additionally be assigned to a better-defined selenide environment, i.e., less non-selenide environments, similar to previous results on KF-PDT absorber surfaces.[9]

Finally, the Ga 3d/In 4d spectral region is investigated in Fig. 4(c). Upon PDT, the Ga 3d signal at ∼20 eV narrows and the In 4d signal at ∼18 eV increases in intensity. This is visible in the difference spectrum, which shows negative intensity at the Ga 3d position and positive intensity at the In 4d position. The former can directly be ascribed to the removal of surface Ga-oxides, as discussed above. A fit was used to quantify the changes. Ga 3d and In 4d are very close to the valence band, exhibiting a weak band dispersion that depends on the specific compound. For our intensity (area) quantification, we neglect this dispersion and describe both Ga 3d and In 4d signals by a spin–orbit split doublet using symmetric Voigt line profiles. A linear background and two Ga 3d and In 4d doublets (to account for the CIGSe and oxidic environments) were used. The area ratio of the doublets was fixed according to the multiplicity 2j + 1, the spin–orbit splitting was used as a fitting parameter, and the relative Gaussian and Lorentzian contributions were kept constant. The simultaneous fit results derive a spin–orbit splitting of 0.41 and 0.76 eV for Ga 3d and In 4d, respectively. Using the respective photoionization cross sections,[57] we derive a GGI surface ratio of 0.94 and 0.93 for no PDT and PDT, respectively (absolute GGI values ± 0.03, relative variations ± 0.01). This GGI value is in line with the laboratory-based data and slightly larger than the GGI value of 0.90 derived from bulk-sensitive x-ray fluorescence.[30] The Ga/Se ratio is reduced by 7% after PDT, which is significantly less than in previous studies of low(er) bandgap KF-PDT CIGSe absorbers which, in some cases, found a strong reduction of Ga at the surface after PDT.[10,44] The parallel PDT-induced increase in the In/Se ratio by 22% leads to an "In-richer" absorber surface. A higher In surface content has been shown to be a key parameter to increase the solar cell performance and possibly facilitate the here-observed efficiency increase.[58]

In summary, we have studied the chemical structure of a GGI = 0.9 CIGSe absorber surface with and without RbF-PDT, using electron spectroscopy (HAXPES, XPS, and XAES). After the PDT, we find (only) small amounts of Rb at the absorber surface, using the unique information from the Rb 2p peak (only accessible with HAXPES). Furthermore, this step leads to a reduction of the Na concentration and removes oxides from the absorber surface. While the amount of Ga at the surface is slightly reduced, the amount of In is slightly increased. We find no spectral evidence for the formation of a purely Rb–In–Se bonding environment. Moreover, the PDT slightly reduces the (downward) band bending toward the absorber surface, in contrast to GGI ∼0.3 absorbers.

In comparison to high-efficiency CIGSe absorbers with GGI ∼0.3 and RbF-PDT, we find some similarities but also significant differences, indicating that the RbF-PDT does not modify the high GGI surface as substantially as for CIGSe absorbers with GGI ∼0.3. While both standard- and high-GGI absorbers show a decrease in Na concentration after PDT,[7,8] the high-GGI absorber shows no copper depletion at the surface. Even though literature sometimes reports on a separate alkali-In–Se surface environment, we do not find such a bonding environment for the high-GGI absorber surface, which is possibly a result of the small Rb and In amounts. This is in agreement with Taguchi *et al.*, who reported that the presence of In is necessary

for the beneficial effects of RbF-PDT.[16] However, the RbF-PDT induced increase in the In content might play a role in the observed PCE improvement. Tuning the GGI at the outermost absorber surface for subsequent RbF treatments could thus open new pathways toward an insight-based optimization of surface treatments for wide-gap CIGSe absorbers and their applications, e.g., in tandem device architectures.

The authors thank the German Federal Ministry for Economic Affairs and Climate Action (BMWK) for funding the "EFFCIS-II" project (Nos. 03EE1059A and 03EE1059E). D. Hauschild, L. Weinhardt, and C. Heske gratefully acknowledge the Deutsche Forschungsgemeinschaft (DFG) for funding in Project Nos. GZ:INST 121384/64-1 FUGG, GZ: INST 121384/65-1 FUGG, and GZ:INST 121384/66-1 FUGG.

AUTHOR DECLARATIONS

Conflict of Interest

The authors have no conflicts to disclose.

Author Contributions

Luisa Both: Data curation (lead); Formal analysis (equal); Investigation (equal); Software (equal); Visualization (lead); Writing – original draft (equal). **Dirk Hauschild:** Conceptualization (equal); Data curation (equal); Formal analysis (equal); Funding acquisition (equal); Investigation (equal); Methodology (equal); Project administration (equal); Software (equal); Supervision (equal); Visualization (equal); Writing – original draft (equal); Writing – review & editing (equal). **Mary Blankenship:** Data curation (equal); Investigation (equal); Validation (equal); Writing – review & editing (equal). **Ralph Steininger:** Data curation (equal); Investigation (equal); Writing – review & editing (equal). **Wolfram Witte:** Funding acquisition (equal); Investigation (equal); Methodology (equal); Project administration (equal); Resources (equal); Writing – review & editing (equal). **Dimitrios Hariskos:** Investigation (equal); Methodology (equal); Resources (equal); Writing – review & editing (equal). **Stefan Paetel:** Investigation (equal); Methodology (equal); Resources (equal); Writing – review & editing (equal). **Michael Powalla:** Conceptualization (equal); Funding acquisition (equal); Resources (equal); Writing – review & editing (equal). **Clemens Heske:** Conceptualization (equal); Formal analysis (equal); Funding acquisition (equal); Resources (equal); Supervision (equal); Validation (equal); Writing – review & editing (equal). **Lothar Weinhardt:** Conceptualization (equal); Formal analysis (equal); Funding acquisition (equal); Resources (equal); Supervision (equal); Validation (equal); Writing – review & editing (equal).

DATA AVAILABILITY

The data that support the findings of this study are available from the corresponding author upon reasonable request.

REFERENCES

[1]M. Nakamura, K. Yamaguchi, Y. Kimoto, Y. Yasaki, T. Kato, and H. Sugimoto, "Cd-free Cu(In,Ga)(Se,S)$_2$ thin-film solar cell with record efficiency of 23.35%," IEEE J. Photovoltaics **9**(6), 1863–1867 (2019).
[2]M. A. Green, E. D. Dunlop, M. Yoshita, N. Kopidakis, K. Bothe, G. Siefer, and X. Hao, "Solar cell efficiency tables (Version 62)," Prog. Photovoltaics **31**(7), 651–663 (2023).
[3]J. Keller, K. Kiselman, O. Donzel-Gargand, N. M. Martin, M. Babucci, O. Lundberg, E. Wallin, L. Stolt, and M. Edoff, "High-concentration silver alloying and steep back-contact gallium grading enabling copper indium gallium selenide solar cell with 23.6% efficiency," Nat. Energy **9**, 467–478 (2024).
[4]P. Jackson, R. Wuerz, D. Hariskos, E. Lotter, W. Witte, and M. Powalla, "Effects of heavy alkali elements in Cu(In,Ga)Se$_2$ solar cells with efficiencies up to 22.6%," Phys. Status Solidi RRL **10**(8), 583–586 (2016).
[5]S. Siebentritt, E. Avancini, M. Bär, J. Bombsch, E. Bourgeois, S. Buecheler, R. Carron, C. Castro, S. Duguay, R. Félix, E. Handick, D. Hariskos, V. Havu, P. Jackson, H. Komsa, T. Kunze, M. Malitckaya, R. Menozzi, M. Nesladek, N. Nicoara, M. Puska, M. Raghuwanshi, P. Pareige, S. Sadewasser, G. Sozzi, A. N. Tiwari, S. Ueda, A. Vilalta-Clemente, T. P. Weiss, F. Werner, R. G. Wilks, W. Witte, and M. H. Wolter, "Heavy alkali treatment of Cu(In,Ga)Se$_2$ solar cells: Surface versus bulk effects," Adv. Energy Mater. **10**(8), 1903752 (2020).
[6]P. Jackson, D. Hariskos, R. Wuerz, O. Kiowski, A. Bauer, T. M. Friedlmeier, and M. Powalla, "Properties of Cu(In,Ga)Se$_2$ solar cells with new record efficiencies up to 21.7%," Phys. Status Solidi RRL **9**(1), 28–31 (2015).
[7]D. Hauschild, D. Kreikemeyer-Lorenzo, P. Jackson, T. M. Friedlmeier, D. Hariskos, F. Reinert, M. Powalla, C. Heske, and L. Weinhardt, "Impact of a RbF postdeposition treatment on the electronic structure of the CdS/Cu(In,Ga)Se$_2$ heterojunction in high-efficiency thin-film solar cells," ACS Energy Lett. **2**(10), 2383–2387 (2017).
[8]D. Kreikemeyer-Lorenzo, D. Hauschild, P. Jackson, T. M. Friedlmeier, D. Hariskos, M. Blum, W. Yang, F. Reinert, M. Powalla, C. Heske, and L. Weinhardt, "Rubidium fluoride post-deposition treatment: Impact on the chemical structure of the Cu(In,Ga)Se$_2$ surface and CdS/Cu(In,Ga)Se$_2$ interface in thin-film solar cells," ACS Appl. Mater. Interfaces **10**(43), 37602–37608 (2018).
[9]M. Mezher, L. M. Mansfield, K. Horsley, M. Blum, R. Wieting, L. Weinhardt, K. Ramanathan, and C. Heske, "KF post-deposition treatment of industrial Cu(In,Ga)(S,Se)$_2$ thin-film surfaces: Modifying the chemical and electronic structure," Appl. Phys. Lett. **111**(7), 071601 (2017).
[10]A. Chirilă, P. Reinhard, F. Pianezzi, P. Bloesch, A. R. Uhl, C. Fella, L. Kranz, D. Keller, C. Gretener, H. Hagendorfer, D. Jaeger, R. Erni, S. Nishiwaki, S. Buecheler, and A. N. Tiwari, "Potassium-induced surface modification of Cu(In,Ga)Se$_2$ thin films for high-efficiency solar cells," Nat. Mater. **12**(12), 1107–1111 (2013).
[11]S. Ishizuka, N. Taguchi, J. Nishinaga, Y. Kamikawa, S. Tanaka, and H. Shibata, "Group III elemental composition dependence of RbF postdeposition treatment effects on Cu(In,Ga)Se$_2$ thin films and solar cells," J. Phys. Chem. C **122**(7), 3809–3817 (2018).
[12]F. Pianezzi, P. Reinhard, A. Chirilă, B. Bissig, S. Nishiwaki, S. Buecheler, and A. N. Tiwari, "Unveiling the effects of post-deposition treatment with different alkaline elements on the electronic properties of CIGS thin film solar cells," Phys. Chem. Chem. Phys. **16**(19), 8843 (2014).
[13]H. Tangara, S. Zahedi-Azad, J. Not, J. Schick, A. Lafuente-Sampietro, M. M. Islam, R. Scheer, and T. Sakurai, "Study of defect properties and recombination mechanism in rubidium treated Cu(In,Ga)Se$_2$ solar cells," J. Appl. Phys. **129**(18), 183108 (2021).
[14]N. Maticiuc, T. Kodalle, J. Lauche, R. Wenisch, T. Bertram, C. A. Kaufmann, and I. Lauermann, "In vacuo XPS investigation of Cu(In,Ga)Se$_2$ surface after RbF post-deposition treatment," Thin Solid Films **665**, 143–147 (2018).
[15]J. Bombsch, E. Avancini, R. Carron, E. Handick, R. Garcia-Diez, C. Hartmann, R. Félix, S. Ueda, R. G. Wilks, and M. Bär, "NaF/RbF-treated Cu(In,Ga)Se$_2$ thin-film solar cell absorbers: Distinct surface modifications caused by two different types of rubidium chemistry," ACS Appl. Mater. Interfaces **12**(31), 34941–34948 (2020).
[16]N. Taguchi, S. Tanaka, and S. Ishizuka, "Direct insights into RbInSe$_2$ formation at Cu(In,Ga)Se$_2$ thin film surface with RbF postdeposition treatment," Appl. Phys. Lett. **113**(11), 113903 (2018).
[17]N. Nicoara, T. Kunze, P. Jackson, D. Hariskos, R. F. Duarte, R. G. Wilks, W. Witte, M. Bär, and S. Sadewasser, "Evidence for chemical and electronic nonuniformities in the formation of the interface of RbF-treated Cu(In,Ga)Se$_2$ with CdS," ACS Appl. Mater. Interfaces **9**(50), 44173–44180 (2017).
[18]F. Larsson, N. S. Nilsson, J. Keller, C. Frisk, V. Kosyak, M. Edoff, and T. Törndahl, "Record 1.0 V open-circuit voltage in wide band gap chalcopyrite solar cells," Prog. Photovoltaics Res. Appl. **25**(9), 755–763 (2017).
[19]S. Ishizuka, "CuGaSe$_2$ thin film solar cells: Challenges for developing highly efficient wide-gap chalcopyrite photovoltaics," Phys. Status Solidi A **216**(15), 1800873 (2019).

[20]W. Shockley and H. J. Queisser, "Detailed balance limit of efficiency of p-n junction solar cells," J. Appl. Phys. **32**(3), 510–519 (1961).
[21]B. Ehrler, E. M. Hutter, and J. J. Berry, "The complicated morality of named inventions," ACS Energy Lett. **6**(2), 565–567 (2021).
[22]R. Herberholz, V. Nadenau, U. Rühle, C. Köble, H. W. Schock, and B. Dimmler, "Prospects of wide-gap chalcopyrites for thin film photovoltaic modules," Sol. Energy Mater. Sol. Cells **49**(1), 227–237 (1997). (97)00199–2.
[23]M. A. Contreras, L. M. Mansfield, B. Egaas, J. Li, M. Romero, R. Noufi, E. Rudiger-Voigt, and W. Mannstadt, "Wide bandgap Cu(In,Ga)Se_2 solar cells with improved energy conversion efficiency," Prog. Photovoltaics Res. Appl. **20**(7), 843–850 (2012).
[24]R. Klenk, "Characterisation and modelling of chalcopyrite solar cells," Thin Solid Films **387**(1–2), 135–140 (2001).
[25]M. Gloeckler and J. R. Sites, "Efficiency limitations for wide-band-gap chalcopyrite solar cells," Thin Solid Films **480–481**, 241–245 (2005).
[26]J. Keller, K. V. Sopiha, O. Stolt, L. Stolt, C. Persson, J. J. S. Scragg, T. Törndahl, and M. Edoff, "Wide-gap (Ag,Cu)(In,Ga)Se_2 solar cells with different buffer materials—A path to a better heterojunction," Prog. Photovoltaics **28**(4), 237–250 (2020).
[27]S. Zahedi-Azad, M. Maiberg, R. Clausing, and R. Scheer, "Influence of heavy alkali post deposition treatment on wide gap Cu(In,Ga)Se_2," Thin Solid Films **669**, 629–632 (2019).
[28]S. Zahedi-Azad, M. Maiberg, and R. Scheer, "Effect of Na-PDT and KF-PDT on the photovoltaic performance of wide bandgap Cu (In,Ga)Se_2 solar cells," Prog. Photovoltaics **28**(11), 1146–1157 (2020).
[29]Y.-H. Chang, R. Carron, M. Ochoa, A. N. Tiwari, J. R. Durrant, and L. Steier, "Impact of RbF and NaF postdeposition treatments on charge carrier transport and recombination in Ga-graded Cu(In,Ga)Se_2 solar cells," Adv. Funct. Mater. **31**(40), 2103663 (2021).
[30]M. Blankenship, D. Hauschild, L. Both, E. Pyatenko, W. Witte, D. Hariskos, S. Paetel, M. Powalla, L. Weinhardt, and C. Heske, "Conduction band cliff at the CdS/$CuIn_{0.1}Ga_{0.9}Se_2$ thin-film solar cell interface," J. Phys. Chem. C **128**(1), 339–345 (2024).
[31]M. Morkel, L. Weinhardt, B. Lohmüller, C. Heske, E. Umbach, W. Riedl, S. Zweigart, and F. Karg, "Flat conduction-band alignment at the CdS/$CuInSe_2$ thin-film solar-cell heterojunction," Appl. Phys. Lett. **79**(27), 4482–4484 (2001).
[32]R. Gutzler, W. Witte, A. Kanevce, D. Hariskos, and S. Paetel, "V_{OC}-losses across the band gap: Insights from a high-throughput inline process for CIGS solar cells," Prog. Photovoltaics Res. Appl. **31**(10), 1023–1031 (2023).
[33]V. Probst, J. Rimmasch, W. Riedl, W. Stetter, J. Holz, H. Harms, F. Karg, and H. W. Schock, "The impact of controlled sodium incorporation on rapid thermal processed Cu(InGa)Se_2-thin films and devices," in *IEEE Photovoltaic Specialists Conference—1994, 1994 IEEE First World Conference on Photovoltaic Energy Conversion, 1994, Conference Record of the Twenty Fourth* (IEEE, 1994), Vol. 1, pp. 144–147. .
[34]C. Heske, R. Fink, E. Umbach, W. Riedl, and F. Karg, "Na-induced effects on the electronic structure and composition of Cu(In,Ga)Se_2 thin-film surfaces," Appl. Phys. Lett. **68**(24), 3431–3433 (1996).
[35]A. Vilalta-Clemente, M. Raghuwanshi, S. Duguay, C. Castro, E. Cadel, P. Pareige, P. Jackson, R. Wuerz, D. Hariskos, and W. Witte, "Rubidium distribution at atomic scale in high efficient Cu(In,Ga)Se_2 thin-film solar cells," Appl. Phys. Lett. **112**(10), 103105 (2018).
[36]M. Raghuwanshi, A. Vilalta-Clemente, C. Castro, S. Duguay, E. Cadel, P. Jackson, D. Hariskos, W. Witte, and P. Pareige, "Influence of RbF post deposition treatment on heterojunction and grain boundaries in high efficient (21.1%) Cu(In,Ga)Se_2 solar cells," Nano Energy **60**, 103–110 (2019).
[37]L. Weinhardt, D. Hauschild, and C. Heske, "Surface and interface properties in thin-film solar cells: Using soft X-rays and electrons to unravel the electronic and chemical structure," Adv. Mater. **31**(26), 1806660 (2019).
[38]L. Weinhardt, R. Steininger, D. Kreikemeyer-Lorenzo, S. Mangold, D. Hauschild, D. Batchelor, T. Spangenberg, and C. Heske, "X-SPEC: A 70 eV to 15 keV undulator beamline for X-ray and electron spectroscopies," J. Synchrotron Radiat. **28**(2), 609–617 (2021).
[39]J. F. Moulder, W. F. Stickle, P. E. Sobol, and K. D. Bomben, *Handbook of X-Ray Photoelectron Spectroscopy* (Physical Electronics Division, Perkin-Elmer Corporation, 1992).
[40]S. Tanuma, C. J. Powell, and D. R. Penn, "Calculations of electron inelastic mean free paths. V. Data for 14 organic compounds over the 50–2000 eV range," Surf. Interface Anal. **21**(3), 165–176 (1994).
[41]S. Tougaard, see http://www.quases.com/home/ for "QUASES (QUantitative Analysis of Surfaces by Electron Spectroscopy)" (2024).
[42]P. Pistor, D. Greiner, C. A. Kaufmann, S. Brunken, M. Gorgoi, A. Steigert, W. Calvet, I. Lauermann, R. Klenk, T. Unold, and M.-C. Lux-Steiner, "Experimental indication for band gap widening of chalcopyrite solar cell absorbers after potassium fluoride treatment," Appl. Phys. Lett. **105**(6), 063901 (2014).
[43]B. Ümsür, W. Calvet, A. Steigert, I. Lauermann, M. Gorgoi, K. Prietzel, D. Greiner, C. A. Kaufmann, T. Unold, and M. C. Lux-Steiner, "Investigation of the potassium fluoride post deposition treatment on the CIGSe/CdS interface using hard X-ray photoemission spectroscopy—A comparative study," Phys. Chem. Chem. Phys. **18**(20), 14129–14138 (2016).
[44]E. Handick, P. Reinhard, R. G. Wilks, F. Pianezzi, T. Kunze, D. Kreikemeyer-Lorenzo, L. Weinhardt, M. Blum, W. Yang, M. Gorgoi, E. Ikenaga, D. Gerlach, S. Ueda, Y. Yamashita, T. Chikyow, C. Heske, S. Buecheler, A. N. Tiwari, and M. Bär, "Formation of a K—In—Se surface species by NaF/KF postdeposition treatment of Cu(In,Ga)Se_2 thin-film solar cell absorbers," ACS Appl. Mater. Interfaces **9**(4), 3581–3589 (2017).
[45]M. Mezher, L. M. Mansfield, K. Horsley, W. Yang, M. Blum, L. Weinhardt, K. Ramanathan, and C. Heske, "Variations in the chemical and electronic impact of post-deposition treatments on Cu(In,Ga)$(S,Se)_2$ absorbers," ACS Appl. Energy Mater. **2**(12), 8641–8648 (2019).
[46]T. Kodalle, M. D. Heinemann, D. Greiner, H. A. Yetkin, M. Klupsch, C. Li, P. A. Aken, I. van; Lauermann, R. Schlatmann, and C. A. Kaufmann, "Elucidating the mechanism of an RbF post deposition treatment in CIGS thin film solar cells," Sol. RRL **2**(9), 1800156 (2018).
[47]D. Hauschild, R. Steininger, D. Hariskos, W. Witte, S. Tougaard, C. Heske, and L. Weinhardt, "Using the inelastic background in hard X-ray photoelectron spectroscopy for a depth-resolved analysis of the CdS/Cu(In,Ga)Se_2 interface," J. Vac. Sci. Technol., A **39**(6), 063216 (2021).
[48]E. Pyatenko, D. Hauschild, V. Mikhnych, R. Edla, R. Steininger, D. Hariskos, W. Witte, M. Powalla, C. Heske, and L. Weinhardt, "Rb diffusion and oxide removal at the RbF-treated Ga_2O_3/Cu(In,Ga)Se_2 interface in thin-film solar cells," ACS Appl. Mater. Interfaces **15**(45), 53113–53121 (2023).
[49]D. W. Niles, "Na impurity chemistry in photovoltaic CIGS thin films: Investigation with x-ray photoelectron spectroscopy," J. Vac. Sci. Technol., A **15**(6), 3044 (1997).
[50]M. Ruckh, D. Schmid, M. Kaiser, R. Schäffler, T. Walter, and H. W. Schock, "Influence of substrates on the electrical properties of Cu(In,Ga)Se_2 thin films," Sol. Energy Mater. Sol. Cells **41–42**, 335–343 (1996).
[51]A. Kylner, "The chemical bath deposited CdS/Cu(In,Ga)Se_2 interface as revealed by X-ray photoelectron spectroscopy," J. Electrochem. Soc. **146**(5), 1816–1823 (1999).
[52]D. Hauschild, F. Meyer, S. Pohlner, R. Lechner, R. Dietmüller, J. Palm, C. Heske, L. Weinhardt, and F. Reinert, "Impact of environmental conditions on the chemical surface properties of Cu(In,Ga)$(S,Se)_2$ thin-film solar cell absorbers," J. Appl. Phys. **115**(18), 183707 (2014).
[53]A. Naumkin, A. Kraut-Vass, S. Gaarenstroom, and C. Powell, see http://srdata.nist.gov/xps/Default.aspx for "NIST X-ray photoelectron spectroscopy (XPS) Database, Version 5.0. NIST X-ray photoelectron spectroscopy (XPS) database, version 5.0" (2023).
[54]D. Schmid, M. Ruckh, and H. W. Schock, "Photoemission studies on Cu(In,Ga)Se_2 thin films and related binary selenides," Appl. Surf. Sci. **103**(4), 409–429 (1996).
[55]M. Faur, M. Faur, D. T. Jayne, M. Goradia, and C. Goradia, "XPS investigation of anodic oxides grown on p-type InP," Surf. Interface Anal. **15**(11), 641–650 (1990).
[56]H. Iwakuro, C. Tatsuyama, and S. Ichimura, "XPS and AES studies on the oxidation of layered semiconductor GaSe," Jpn. J. Appl. Phys., Part 1 **21**(1R), 94 (1982).
[57]M. B. Trzhaskovskaya, V. I. Nefedov, and V. G. Yarzhemsky, "Photoelectron angular distribution parameters for elements Z=1 to Z=54 in the photoelectron energy range 100–5000 eV," At. Data Nucl. Data Tables **77**(1), 97–159 (2001).
[58]M. Bär, I. Repins, M. A. Contreras, L. Weinhardt, R. Noufi, and C. Heske, "Chemical and electronic surface structure of 20%-efficient Cu(In,Ga)Se_2 thin film solar cell absorbers," Appl. Phys. Lett. **95**(5), 052106 (2009).